

RECENT DEVELOPMENTS IN THE NIST CRYOGENIC THERMAL TRANSFER STANDARD PROJECT

Speaker: Thomas E. Lipe
National Institute of Standards and Technology
100 Bureau Drive, Mail Stop 8111
Gaithersburg, MD 20899-8111
Phone: 301.975.4251
FAX: 301.926.3972
Email: thomas.lipe@nist.gov

Paper Author(s): Thomas E. Lipe*, Joseph R. Kinard*, and Carl D. Reintsema[†]
Electronics and Electrical Engineering Laboratory
National Institute of Standards and Technology

ABSTRACT

We describe the development of a Cryogenic Thermal Transfer Standard (CTTS) from the first prototype in 1997 to the present version. A description of the superconducting transition-edge sensor and the development of a superconducting input transmission line are given. We also present data demonstrating the performance of the CTTS.

I. INTRODUCTION

The most accurate RMS measurements of voltage and current are made by comparing the heating effect of an unknown ac signal to that of a known dc signal using a thermal converter. Thermal converters are usually composed of one or more thermocouples arranged along a heater structure, generally a wire or thin-film conductor^(1,2). The most accurate thermal converters are multijunction thermal converters⁽³⁾, which are used at most National Measurement Institutes as the basis for ac voltage and current calibrations. The limiting factors for the accuracy of these thermal converters at low voltages and audio frequencies are, to a great extent, thermal and thermoelectric effects that are temperature dependent⁽⁴⁾. We are developing a thermal transfer standard that operates at temperatures below 10 K, where these thermal effects are expected to be quite small. The Cryogenic Thermal Transfer Standard (CTTS) is especially suitable for use at extremely small input power levels, where an accurate primary standard does not as yet exist. It is hoped that this effort will eventually lead to the introduction of a new class of primary standard for ac-dc difference calibrations, with uncertainties an order of magnitude less than present primary standards.

Contribution of the U.S. Government. Not subject to copyright in the United States.

* Electricity Division, Gaithersburg, MD

[†] Electromagnetic Technology Division, Boulder, CO

NIST is part of the Technology Administration, U.S. Department of Commerce.

2001 NCSL International Workshop & Symposium

II. THEORY OF OPERATION

The CTTS operates on a power substitution principle illustrated in simplified form in Fig. 1. The total power at the converter thermal node, P_{total} , is

$$P_{total} = P_{trim} + P_{signal} \quad (1)$$

where P_{trim} is the power supplied to the trim resistor and P_{signal} is the power in the signal heater.

As the power in the signal resistor changes (for example, when the signal is switched from ac to dc or vice-versa), the total power at the converter node is kept constant by adjusting the power in the trim resistor, so that

$$\Delta P_{signal} = -\Delta P_{trim} \quad (2)$$

By monitoring the voltage supplied to the trim resistor, the ac-dc difference, δ , of the CTTS in parts in 10^6 may be determined from

$$\delta = \frac{Q_{ac} - Q_{dc}}{Q_{dc}} \times 10^6 \quad (3)$$

where Q_{ac} is the ac quantity of interest and Q_{dc} is the average of the two polarities of dc input that produces the same output from the thermal converter as that produced by Q_{ac} . Since very small changes in the input signal power (and hence the temperature of the thermal node) create large changes in the resistance of the transition-edge sensor (TES), this technology has the potential to be a very powerful method of measuring ac-dc differences. As shown in Table 1, the sensitivity of the TES is several orders of magnitude greater than that of an ordinary thermocouple.

The resistance of the TES is monitored using an ac resistance bridge with an integrated temperature controller. The temperature controller uses a Proportional-Integral-Derivative (PID) control algorithm to supply the power to the trim heater necessary to maintain the appropriate thermal node at a temperature determined by the critical temperature (T_c) of the TES. In practice a separate resistance bridge/temperature controller combination is used to control each of the two thermal nodes (the converter stage and the reference platform) in the CTTS.

III. DESIGN

An important concern in the design of the CTTS is to minimize the flow of heat onto the thermal converter. The T_c of the niobium-tantalum (NbTa) alloy of the TES is about 6 K, with a transition region about 3 mK wide. The cold plate of the cryostat is maintained by liquid helium at 4 K; therefore the thermal converter must be partially isolated thermally from the cold plate. This partial thermal isolation must be sufficient to maintain the converter in its transition region without supplying much power (and therefore heat), but must still allow the converter to cool in a reasonable time. This is accomplished by placing the converter thermal node on, and slightly

thermally isolated from, a reference platform (indicated by the platform thermal node in Fig. 1) that is secured to the cold plate by four stainless steel legs. The reference platform employs a 3.75 k Ω phosphor-bronze heater and TES chip, which is used to control the temperature of the reference platform to about 6 K, or just below the T_c of the converter-stage TES.

Both the reference platform and thermal converter stage employ a TES chip, shown in Fig. 2. On each of the 1-cm square chips is a TES, a 7 Ω gold signal heater, and a 450 Ω palladium-gold trim heater. The TES chips are epoxied to molybdenum disks (to match the thermal expansion of the silicon substrate), which are in turn mounted to the gold-plated, oxygen-free high-purity copper (OFHC) platforms. Signals from the ac bridges and temperature controllers are carried to the converter stages via niobium (Nb) ribbons, bonded to pads on both the TES and heaters at one end and bonded to tracks on circuit board material mounted on the reference platform at the other end. The first prototype⁽⁵⁾ featured a TES fabricated from Nb; however, the T_c of Nb is about 9 K, so that the TES and the Nb ribbons had approximately the same T_c . This arrangement is not ideal, since at 9 K the ribbons may not be fully superconducting and their resistance fluctuates with the power applied to the chip, resulting in some heat being conducted onto the converter stage as well as introducing errors due to the variations in the lead resistance. These problems were solved by fabricating subsequent sensors from a NbTa alloy. The Nb ribbons are fully superconducting at the T_c of the NbTa TES, and no heat flows along the ribbons onto the converter stage. The circuit boards on the reference platform route the signals under an OFHC radiation shield to four-pin connectors at the edge of the platform. The bridge measurement and control signal leads are of 0.0127 cm manganin wire, which is thermally anchored to several temperature stages, including the 4 K cold plate of the cryostat, the side of the liquid helium tank, and the liquid nitrogen tank. The signals are passed through the vacuum jacket of the cryostat on hermetically-sealed connectors. A photograph of the reference platform and converter stage is shown in Fig. 3.

IV. NORMAL METAL INPUT TRANSMISSION LINES

In the first prototype of the CTTS, the ac-dc input signal lead was 0.0127 cm twisted-pair manganin wire, about 45 cm long, which was thermally anchored to the liquid nitrogen and liquid helium tanks and to the 4 K cold plate. Although manganin wire of this size is a relatively poor heat conductor, and an appropriate choice for cryogenic applications, it is a rather poor choice for an electrical transmission line owing to its resistance of about 1 Ω /cm. In fact, the ac-dc differences of the CTTS measured using this twisted-pair input lead were extremely large as a voltage converter particularly at high frequencies, due to reactance effects in the leads. This input structure also created large and uncertain voltage drops from the input connector to the converter stage. Measurements made using this input structure are shown in Table 2.

To address the problems associated with the twisted-pair manganin input lead, an input lead based on semi-rigid coaxial cable was designed and installed in the cryostat. Maintaining coaxial symmetry while thermally grounding the outer and inner conductors was accomplished by breaking the cable at two places and routing the conductors across aluminum oxide (alumina) substrates which are normally used to mount thin-film thermal converters⁽⁶⁾. The conductors were soldered to the tabs on the substrate; the substrates were then anchored to the liquid nitrogen tank and 4 K cold plate of the cryostat. The distance from the substrate to the SMA

input connector on the reference platform was spanned by about 4 cm of twisted-pair manganin wire. A photograph of the coaxial transmission line mounted to the cryostat cold plate is shown in Fig. 4

As shown in Table 2, measurements indicated that the coaxial input transmission line was a considerable improvement over the manganin twisted-pair wire. In an attempt to separate the errors arising from thermoelectric (dc) effects on the chip from those ac effects from the transmission line, the CTTS was measured against a Fast-Reversed DC (FRDC) Source⁽⁷⁾ at several switching frequencies. The results (Fig. 5) show that the thermoelectric errors are quite small, indicating that the primary contributions to the ac-dc difference in the CTTS were from ac effects, such as reactance in the input leads. These effects were exacerbated by the 45 cm length of the line which resulted in a lead resistance of about 15 Ω and capacitance of about 2 200 pF.

V. SUPERCONDUCTING INPUT TRANSMISSION LINE

To attempt to reduce the components of ac-dc difference associated with the normal-metal transmission line, a transmission line made of a crystalline thin film of $\text{YBa}_2\text{Cu}_3\text{O}_x$ (YBCO) deposited on a substrate of lanthanum aluminate was fabricated and installed in the cryostat⁽⁸⁾. This structure, shown in Fig. 6, carries the input signal between the 77 K region at the nitrogen shield and the 4 K region inside the helium shield. Since the YBCO is well below its 90 K critical temperature, this transmission line greatly enhances the thermal isolation to the experimental platform while providing better electrical properties than the previous coaxial line. In fact, the input resistance of the CTTS at its operating temperature is approximately 9 Ω , the bulk of which is the 7 Ω signal heater. The remainder of the input resistance is in the tracks that carry the signal under the radiation shield to the converter stage.

To maximize the thermal isolation of the YBCO line from the laboratory environment, a 7 cm extension was fitted to the outside of the cryostat vacuum jacket. This extension contains a high aspect ratio, copper coplanar stripline, patterned on conventional circuit board. This transmission line carries the input signal between the room temperature BNC feedthrough and the 77 K nitrogen shield.

Measurements on the CTTS using the new high- T_c transmission line are presented in Table 2. These measurements show a large improvement over the normal-metal coaxial transmission line as a voltage converter. The voltage level dependence of the CTTS (Table 3) with the YBCO line is rather large, and an indication of the variation of the T_c of the sensor caused by differences in the magnetic field coupling between the signal heater and TES at different heater currents.

Results of measurements on the CTTS as a thermal current converter (TCC) are shown in Table 4. The ac-dc differences of the CTTS as a TCC are fairly independent of frequency relative to the NIST standard TCC; the large differences shown in Table 4 are the result of the large correction to the NIST standard. This data compares favorably with earlier data taken with the twisted-pair manganin input leads, indicating that the ac-dc differences of the CTTS as a TCC are independent of transmission line type, as expected.

VI. CONCLUSIONS AND FUTURE PLANS

We have presented data indicating substantial improvements in the CTTS due to continuing improvements in the input transmission line and control leads. Indications are that this will be a viable approach to a new type of ac-dc primary standard that may prove better than existing standards, especially in the low-power regime. The primary focus of this project in the near term is to address the instability of the measurement process (represented by the large Type A uncertainties). A promising approach is to use PID control software external to the temperature controllers in conjunction with a high-performance dc source to supply a more stable feedback signal to the TES chip. We also plan to add shielding to the chip to isolate the TES from magnetic fields arising from currents in the signal and trim resistors, and to investigate improved resistance measurement techniques.

REFERENCES

- (1) Hermach, F. L., "Thermal converters as ac-dc transfer standards for voltage and current at audio frequencies," *J. Res. Natl. Bur. Stand. (U.S.)*, vol. 48, February 1952, pp. 121-138.
- (2) Inglis, B. D., "Standards for ac-dc transfer," *Metrologia*, vol. 29, January, 1992, pp. 191-199.
- (3) Hermach, F. L., Kinard, J. R., and Hastings, J. R., "Multijunction thermal converters as the NBS primary ac-dc transfer standards for ac current and voltage measurements," *IEEE Trans. Instrum. Meas.*, vol. 36, June 1987, pp. 300-306.
- (4) Hermach, F. L., and Flach, D. R., "An investigation of multijunction thermal converters," *IEEE Trans. Instrum. Meas.*, vol. 25, December, 1976, pp. 524-528.
- (5) Reintsema, C. D., Kinard, J. R., Lipe, T. E., Koch, J. A., and Grossman, E. N., "Thermal Transfer Measurements at Microwatt Power Levels," in *CPEM '98 Conference Digest*, Washington, DC, USA, July 6-10, 1998, pp. 171-172.
- (6) Kinard, J. R., Huang, D. X., and Novotny, D. B., "Performance of Multilayer Thin-Film Multijunction Thermal Converters," *IEEE Trans. Instrum. Meas.*, vol. 44, no. 2, April 1995, pp. 383-386.
- (7) Klonz, M., Hammond, G., Inglis, B. D., Sasaki, H., Speigel, T., Stojanovic, B., Takahashi, K., and Zirpel, R., "Measuring Thermoelectric Effects in Thermal Converters with a Fast Reversed DC," *IEEE Trans. Instrum. Meas.*, vol. 48, no. 2, April 1995, pp. 379-382.
- (8) Reintsema, C.D., Kinard, J. R., and Lipe, T.E., "A High-Temperature Superconducting Transmission Line for Cryogenic Electrical Metrology Applications," in *CPEM 2000 Conference Digest*, Sydney, NSW, Australia, May 14-19, 2000, pp. 488-489.

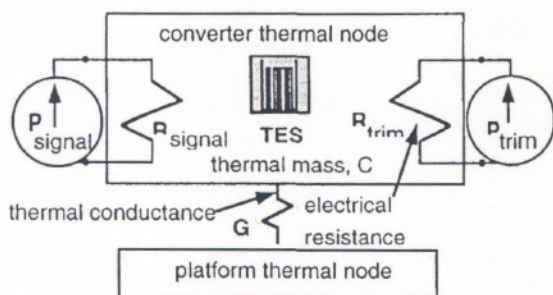


Figure 1. Electrical substitution diagram of the CTTS, showing the signal and trim heaters (R_{signal} and R_{trim}), the transition-edge sensor (TES), and the two thermal nodes.

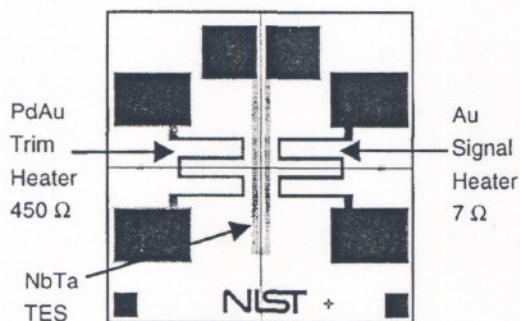


Figure 2. Transition-edge sensor chip. The die size is 1 cm x 1 cm.

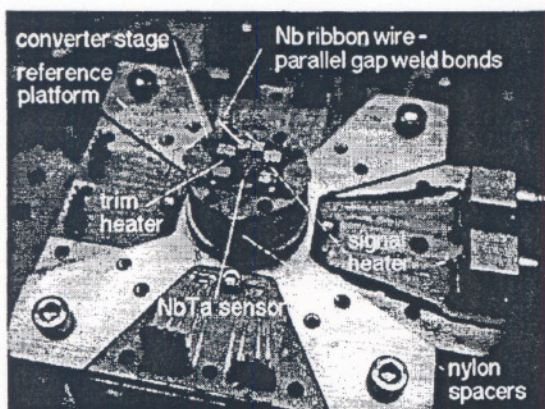


Figure 3. The reference platform and converter stage of the CTTS. The background is the 4 K plate of the cryostat.

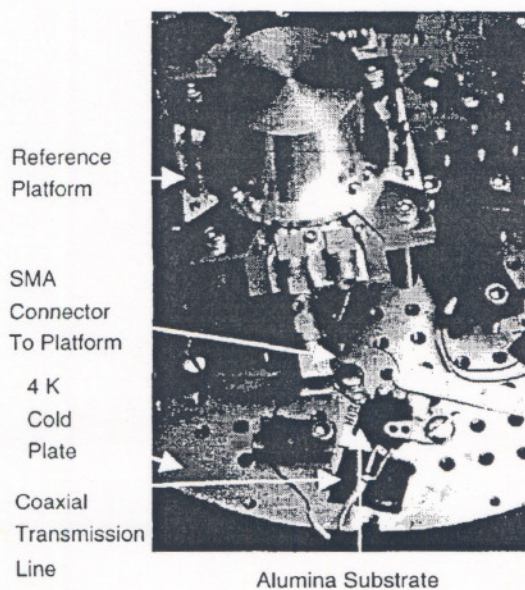


Figure 4. The 4 K cold plate of the cryostat showing the reference platform, coaxial transmission line, and alumina substrate.

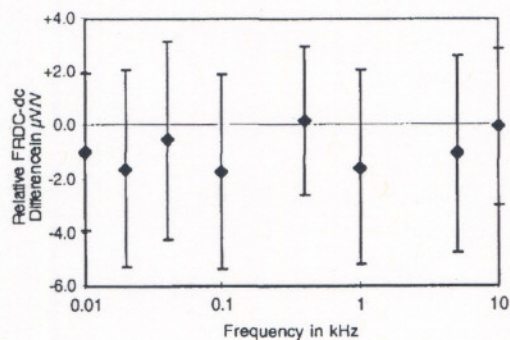


Figure 5. FRDC-dc Difference of the CTTS with the normal-metal input line. Measurement voltage is 15 mV. Uncertainty bars are the $k=2$ Type A uncertainties of the measurement process.

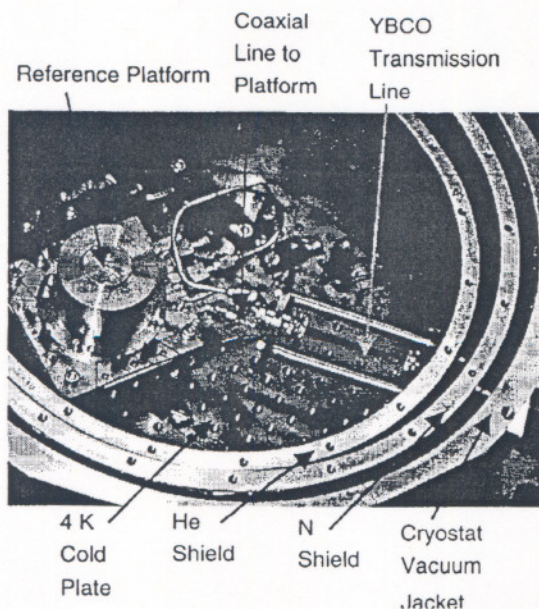


Figure 6. Interior of cryostat showing the YBCO transmission line in its support.

Table 1. Sensitivity of a typical thermocouple compared to a TES. The last row in the table is the logarithmic derivative of the sensitivity.

Thermocouple		TES	
$T - T_{\text{ambient}}$	$\sim 200 \text{ K}$	$T - T_{\text{ambient}}$	$\sim 100 \text{ mK}$
$(dV/dT)_{\text{peak}}$	$100 \mu\text{V/K}$	$(dR/dT)_{\text{peak}}$	$8000 \Omega/\text{K}$
$\frac{T}{V} \left(\frac{dV}{dT} \right)_{\text{peak}}$	< 1	$\frac{T}{R} \left(\frac{dR}{dT} \right)_{\text{peak}}$	~ 3100

Table 2. Ac-dc Differences of the CTTS as a voltage converter with different input transmission structures. The uncertainties are the k=2 Type A uncertainties of the measurement process. *Extrapolated from lower frequencies.

Input Line Type	Ac-dc Difference ($\mu\text{V/V}$)							
	20 Hz	100 Hz	400 Hz	1 kHz	10 kHz	20 kHz	50 kHz	100 kHz
Manganin	-162 ± 4	-162 ± 8		$+70 \pm 8$	$+2620 \pm 10$	$+5463^*$	$+13953^*$	$+28120^*$
Normal Metal Coaxial		-129 ± 7	-187 ± 5	-214 ± 7	$+33 \pm 12$	$+377 \pm 7$	$+956 \pm 7$	$+1647 \pm 6$
YBCO HTS	-204 ± 12	-264 ± 9	-246 ± 9	-227 ± 6	-246 ± 10	-142 ± 12	$+12 \pm 9$	$+362 \pm 6$

Table 3. Voltage level dependence of the CTTS at 1 kHz. The uncertainties are the k=2 Type A uncertainties of the measurement process.

Input Voltage	Ac-dc Difference ($\mu\text{V/V}$)
10 mV	-180 ± 21
14 mV	-228 ± 6
16 mV	-234 ± 9

Table 4. Measurements on the CTTS as a current converter. The uncertainties are the k=2 Type A uncertainties of the measurement process.

Input Current	Ac-dc Difference ($\mu\text{A/A}$)			
	10 kHz	20 kHz	50 kHz	100 kHz
500 μA	$+9 \pm 7$	$+26 \pm 9$	$+98 \pm 7$	$+288 \pm 6$
700 μA	$+2 \pm 4$	$+18 \pm 9$	$+92 \pm 5$	$+285 \pm 7$
1 mA	$+24 \pm 6$	$+41 \pm 3$	$+111 \pm 3$	$+297 \pm 3$